NOAA Technical Memorandum OAR PMEL-151
doi: 10.25923/wdbz-jw97

TSUNAMI INUNDATION MODELING OF THE SAN JUAN ISLANDS, WASHINGTON, DUE TO A CASCADIA SUBDUCTION ZONE EARTHQUAKE

Diego Arcas[1]
Edison Gica[2]
Vasily V. Titov[1]

[1] Pacific Marine Environmental Laboratory (PMEL),
National Oceanic and Atmospheric Administration, Seattle, Washington

[2] Formerly at Joint Institute for the Study of the Atmosphere and Ocean (JISAO),
University of Washington, Seattle, Washington

Pacific Marine Environmental Laboratory
Seattle, Washington
September 2020

UNITED STATES DEPARTMENT OF COMMERCE
Wilbur Ross
Secretary

NATIONAL OCEANIC AND ATMOSPHERIC ADMINISTRATION
Neil A. Jacobs, Ph.D.
Acting Under Secretary for Oceans and Atmosphere

Office of Oceanic and Atmospheric Research
Craig McLean
Assistant Administrator

Contribution 4069 from NOAA Pacific Marine Environmental Laboratory

Also available from the National Technical Information Service (NTIS)

(http://www.ntis.gov)

Contents

List of Figures

List of Tables

Tsunami Inundation Modeling of the San Juan Islands, Washington, due to a Cascadia Subduction Zone Earthquake

D. Arcas[1], E. Gica[2], and V. V. Titov[1]

Abstract. Tsunami inundation modeling for the coastal areas of the San Juan Islands, Washington, due to a great earthquake along the Cascadia subduction zone was conducted using a single earthquake source scenario and a high-resolution inundation model. Simulated results showed that the initial tsunami wave peak hits the southern coast of the San Juan Islands more than 1.25 hours after the earthquake, with tsunami flow depths higher than 3 meters occurring at certain coastal areas. The simulation also showed high current speeds in channels between the islands. The results of this study can be used to enhance the State of Washington's mitigation efforts for the San Juan Islands.

1 NOAA Center for Tsunami Research, Pacific Marine Environmental Laboratory (PMEL), NOAA, Seattle, WA

2 Formerly at University of Washington, Joint Institute for the Study of the Atmosphere and Ocean, Seattle, WA

1. Background

Based on paleoseismic records and the study of turbidities along the continental margin, it is now well established that the Cascadia Subduction Zone (CSZ) has experienced a number of recurring great earthquakes over the last 10,000 years (Atwater and Hemphill-Haley, 1997; Graehl et al., 2015; Kelsey et al., 2005; Nelson et al., 2006; Witter et al., 2003). Noting the prevalence of turbidity sediments in the central and southern part of the CSZ margin, this region appears to be more seismically active than the northern sector of the subduction zone (Goldfinger et al., 2012). However, there is also evidence from turbidities and other records of large earthquakes with magnitudes 9.0 or larger, rupturing the entire length of the subduction zone from northern California to Vancouver Island. By combining geology, dendrochronology, radiocarbon, and tsunami modeling studies in addition to Japanese historical records, it has been determined that the most recent of these full margin rupture events occurred along the CSZ in 1700 (Atwater et al., 1995, 2005; Satake et al., 1996, 2003; Yamaguchi et al., 1997). A study by Petersen et al. (2002) determined that the chance of recurrence of such an earthquake within the next half century is between 10 and 14 percent. The magnitude of this great earthquake would be similar to that of the 11 March 2011 Honshu event (Dengler et al., 2011), which caused significant tsunami devastation along the coast of Japan.

The State of Washington is preparing at-risk communities along the Pacific coast for this and other potential events by developing tsunami hazard and evacuation maps. Similar studies for the Washington communities of Long Beach and Ocean Shores have already been conducted (D. Arcas et al., *unpublished study*). The current study is supported by the Washington State Emergency Management Division, to enhance the State's effort in mitigating the effects of tsunami impact for the San Juan Islands.

2. Study Area

The San Juan Islands (**Figure 1**), located at the northeastern end of Puget Sound, are the remnants of mountain tops of a receding continent (McLellan, 1927). There are 172 named islands comprising the San Juan Islands; some are only visible during lower low tide (McLellan, 1927). In total, San Juan County includes over 400 miles of marine shoreline, more than any other US county (Puget Sound Partnership, 2019), with "a mix of sandy and rocky beaches, shallow and deep harbors, and placid and reef-studded bays" (U.S. Congress, 2011). The temperature is moderate, at ~40° F in winter and ~70° F in summer (San Juan Islands Visitors Bureau, 2019). Most of the trees found along the coast are Pacific Madrone *(Arbutus menziesii)* with evergreen fir and pine forests occupying inland areas

Figure 1. Google Earth map of the San Juan Islands, Washington.

(Tucker and King, 2012). The islands are home to pods of Orcas and other marine mammals such as the river otter, steller sea lion, Pacific Harbor seals, and Dall's porpoise (National Park Service, 2019; Puget Sound Partnership, 2019).

Members of six Central Coast Salish tribes, including the Lummi nation, inhabited the islands for thousands of years prior to the arrival of Europeans in the 18th century (National Park Service, 2019; San Juan Islands Visitors Bureau, 2019). The islands became a US territory in 1872, and to protect Bureau of Land Management lands on the islands, President Obama declared the San Juan Islands a national monument on 25 March 2013 (Bureau of Land Management, 2019).

San Juan County covers 173.92 square miles, with a population of 17,582 yielding a population density of 101 persons per square mile (U.S. Census Bureau, 2019). Orcas (57 square miles; Orcas Island Chamber of Commerce, 2019), Lopez

(29.5 square miles), and San Juan (55.3 square miles) are the largest islands in the San Juan archipelago (**Figure 2**). According to the San Juan Islands Visitors Bureau (2019), the majority of its current year-round residents (more than 16,000 people) inhabit the four main ferry-served islands, Lopez (pop. ~2500), Shaw (pop. ~240), Orcas (pop. ~5400; Orcas Island Chamber of Commerce, 2019), and San Juan Island (pop. ~8000).

Orcas Island is rugged and hilly, with the San Juan Islands' highest point, Mt. Constitution, rising 2409 feet above sea level. Lopez Island is relatively flat, with a total shoreline length of 63 miles. San Juan Island features a variety of terrain, from forest to long stretches of farmland and beachfront (San Juan Islands Visitors Bureau, 2019).

The town of Friday Harbor, on the east side of San Juan Island, is the San Juan County seat. The main industry is tourism, with construction, trade (including retail trade), transportation, utilities, government, education, and health services (Vance-Sherman, 2020) also contributing strongly to the islands' economy. The county's per capita personal income in 2018 was $76,749, with a median household income (2014–2018) of $60,711 (Vance-Sherman, 2020).

Figure 2. Closer view of the San Juan Islands showing the locations of San Juan Island, Lopez Island, Orcas Island, Shaw Island, Blakely Island, and certain bays, channels, and sounds (as discussed in section 5.3).

3. Tsunami Source

The scenario selected by Washington State Division of Natural Resources for this study of the San Juan Islands corresponds to a tectonic rupture along the Cascadia subduction zone. It is one of 15 rupture scenarios identified by Witter et al. (2011, 2012, 2013) from turbidite evidence and onshore paleoseismic records. In their study, Witter et al. (2011) recommended the selection of scenarios M1 and L1 for "practical engineering design, building codes and land use planning along the coast." To provide an added level of safety, this study focuses solely on Scenario L1, which (as compared to M2) has a higher maximum and average slip values, as well as a tsunami-amplifying splay fault distributed parallel to the direction of strike, generating a higher moment magnitude, thus resulting in larger tsunami waves.

The extent of earthquake deformation along the Cascadia subduction zone ranges from slightly above 40°N to approximately 49°N. **Figure 3** shows the slip distribution along the U.S. West Coast while **Table 1** lists the tsunami source parameters. The northern end of the source appears truncated due to the lack of seismic modeling results north of 49°N; however, future inundation studies should include slip distribution estimates of the source north of this point when available. This distinction, however, does not seem to affect the amount of tsunami wave energy entering the Strait of Juan de Fuca, and therefore, it is inconsequential to the assessment of tsunami impact on the San Juan Islands.

Table 1: Tsunami source parameters used for San Juan Islands high-resolution inundation model.

Parameter	Scenario L1
Rupture length [km]	1000
Rupture width [km]	83
Average slip [m]	13.0
Maximum slip [m]	27
Moment magnitude	9.0

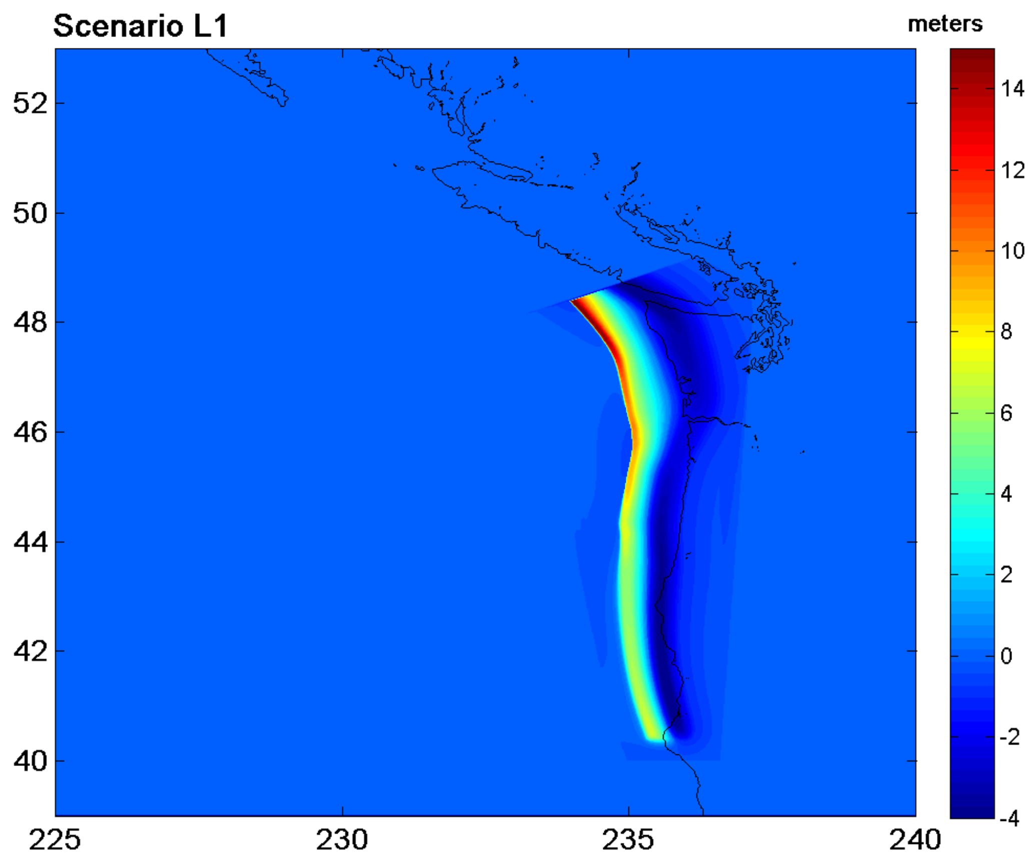

Figure 3. Slip distribution of seismic source scenario L1 along the Cascadia subduction zone (Witter et al., 2011).

4. Tsunami Model

The numerical model used in the simulation, called MOST (Method of Splitting Tsunami), uses a finite difference scheme to solve the nonlinear shallow water equation (Titov and González, 1997). MOST is a suite of numerical simulation codes capable of simulating three processes of tsunami evolution: tsunami generation, transoceanic propagation, and inundation of dry land. The MOST model has been tested extensively against a number of laboratory experiments and benchmarks (Synolakis et al., 2007; Titov and González, 1997; Titov and Synolakis, 1998).

The general methodology to conduct inundation modeling with the MOST numerical code is based on the development of a set of three nested grids, referred to as A, B, and C grids. Each of the grids become successively finer in resolution as they telescope into the community of interest. There are two reasons for the use of grids of increasingly larger resolution. First, in order to numerically resolve a particular wave frequency, a minimum number of nodes per wavelength must be used. As waves travel from deep to shallow water, their wavelengths become smaller due to the fact that the front of the wave, now in shallow water, travels slower than the back of the wave, which is still moving in deep water. As the wavelength shortens, the grid resolution has to be increased to guarantee an approximately constant number of grids nodes per wavelength. The second reason to increase resolution as the wave approaches the study area is related to the resolution of topographic and bathymetric features that may exhibit small length scales in either the vertical or horizontal dimension and, consequently, can disappear from a coarse resolution grid. While these features may have small length scales, they can have a major impact on local wave dynamics. For instance, a breakwater may be a very narrow structure and can easily disappear in a coarse resolution grid, but its presence will have a highly significant impact on wave dynamics by blocking the wave from propagating into certain areas of the domain.

For these reasons, the offshore area is covered by the larger and lower resolution A-grid, and shallow coastal waters are covered with the higher resolution B and C grids. There are, however, cases where a higher resolution grid will still not resolve certain bathymetric features. Using the previous example, a breakwater may not be wide enough to be resolved in a 1/3 arc-second grid, and running a simulation higher than 1/3 arc-second for very large domains may be exceedingly expensive from a computational standpoint. For cases such as these, the breakwater is widened so that it will not disappear from the 1/3 arc-second grid. Increasing the width of the breakwater will have some effect on the simulated waves, but the effect without this modification is significantly greater.

4.1 Digital elevation model development

The digital elevation models (DEMs) used for this study were developed in collaboration with National Geophysical Data Center (NGDC) and are available at https://data.noaa.gov//metaview/page?xml=NOAA/NESDIS/NGDC/MGG/DEM/iso/xml/1961.xml&view=getDataView&header=none. The bathymetric-topographic DEM was constructed with data sources obtained from the NOAA National Oceanic Survey (NOS), Coastal Service Center (CSC), and Office of Coast Survey; Canadian Hydrographic Service (CHS) and Canadian Digital Elevation Data (CDED); Washington State Department of Ecology; Puget Sound Lidar Consortium (PSLC); Moss Landing Marine Laboratory (MLML); and U.S. Geological Survey (USGS). The final product has a grid resolution of 0.4 arc-second with a Mean High Water (MHW) datum for its vertical datum and North American Datum of 1983 for its horizontal datum. The MHW datum is used since the MOST model does not include tidal dynamics, and use of this datum would simulate inundation at high tide. The DEM uses geographic decimal degrees for the coordinate system and has grid extents from 122.5757°W to 124.3633°W and 48.2347°N to 48.875°N, covering the San Juan Islands (**Figure 4**). Details of the development of the 0.4 arc-second DEM are provided in Lim et al. (2011).

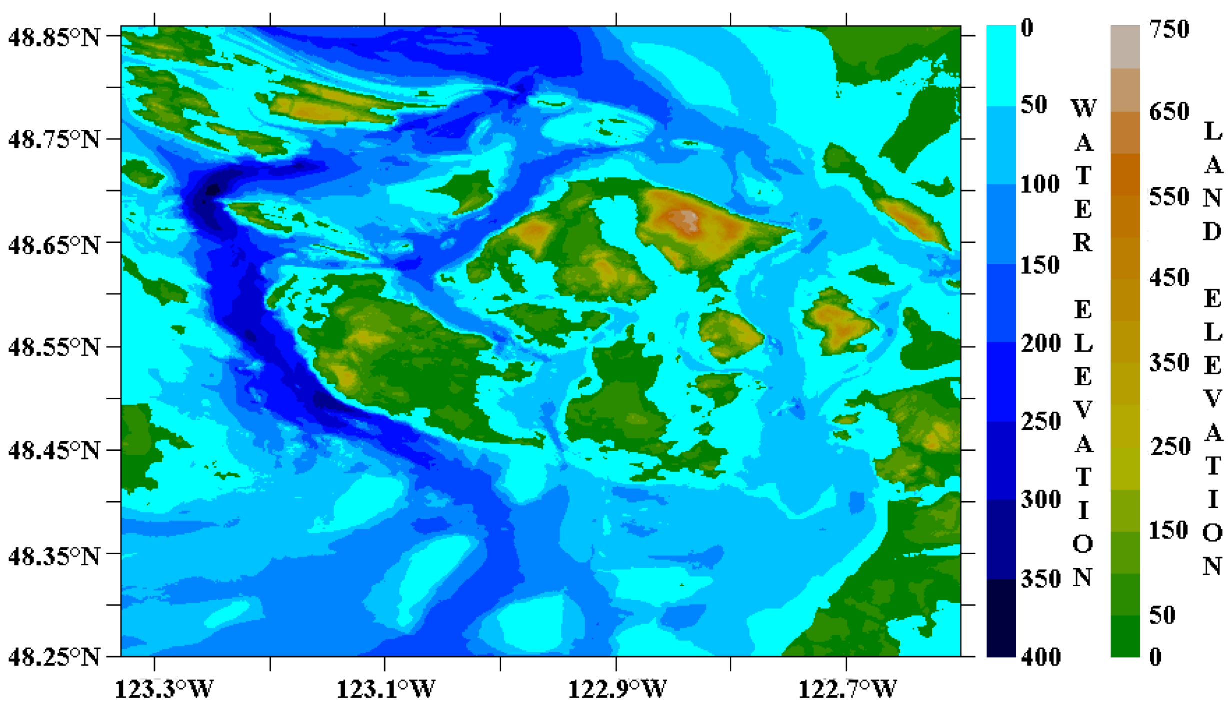

Figure 4. Extent of NGDC 0.4 arc-second digital elevation model for the San Juan Islands.

4.2 Model setup

The DEM for the high-resolution inundation model for San Juan Islands, Washington, is extracted by sub-sampling the 0.4 arc-second grid developed by NGDC (Lim et al., 2011) to construct the A and B grids while preserving the 0.4 arc-second resolution in the C grid. The high-resolution inundation models consist of three nested grids where the outermost grid (A grid) covers the deep ocean region, to capture the tsunami characteristics as it propagates in the deep ocean and into the Strait of Juan de Fuca, and the innermost grid (C grid) covers the San Juan Islands, to capture the tsunami wave transformations in shallow waters and the topography, essential to study inundation and wave interactions between islands. The extent of the 0.4 arc-second DEM developed by NGDC does not cover the grid extents needed by both A and B grids. The A grid is obtained from a 30 arc-second resolution Pacific grid while the B grid is from a 6 arc-second Strait of Juan de Fuca DEM (Venturato et al., 2004). To maintain stability, an algorithm that restricts the variation of the refraction index between two neighboring nodes is applied to the entirety of the computational grids (E. Tolkova, *unpublished study*). However, at times, localized instabilities persist, and these are resolved by manually applying minor modifications on the specific node, or using Matlab cubic smoothing spline within a cluster of nodes if the single node causing the instability is not located.

The coverage extents of the San Juan Islands high-resolution inundation models are provided in **Table 2**. Details of the modeling parameters used for the nested grid (A, B, and C) are included. The coverage extents of the nested grids for the high-resolution inundation model are plotted in **Figures 5–7**.

Table 2: Modeling parameters used for San Juan Islands high-resolution inundation model.

San Juan Islands Grid – Region	Coverage Lat. [°N]	Coverage Lon. [°W]	Cell Size [“]	nx × ny	Time Step [sec]
A – U.S. West Coast	43.0000–52.0000	225.0000–283.0000	30 × 30	1561 × 1081	3.0
B – Strait of Juan de Fuca	47.7525–49.2458	235.0025–237.8958	6 × 6	1737 × 897	1.5
C – San Juan Islands	48.3499–48.8591	236.7399–237.2998	1.2 × 0.8	1675 × 2284	0.3

Minimum offshore depth [m]: 1.0; Water depth for dry land [m]: 0.1; Friction coefficient [n^2]: 0.0009

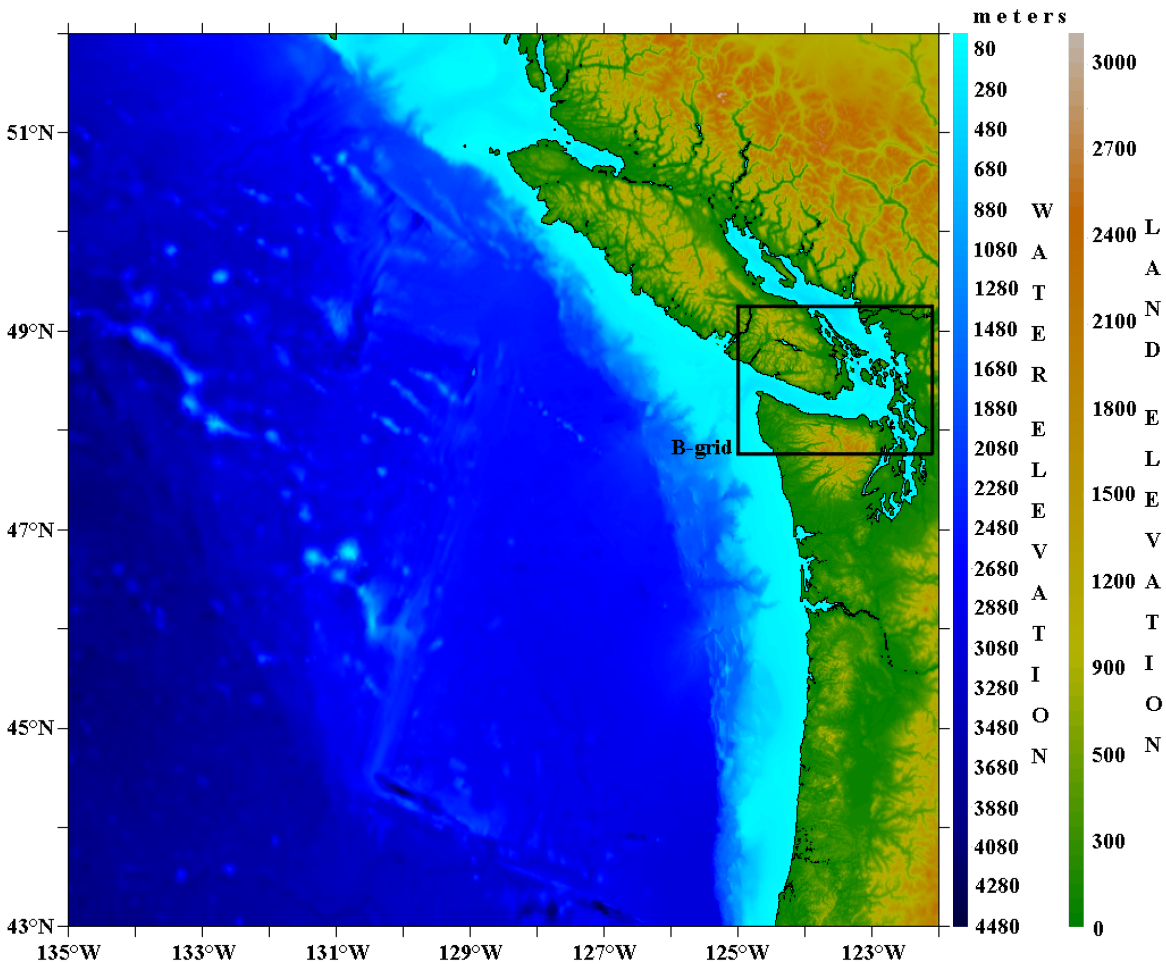

Figure 5. Extent of the A grid used for the San Juan Islands high-resolution inundation model. Black box indicates the extent of the B grid.

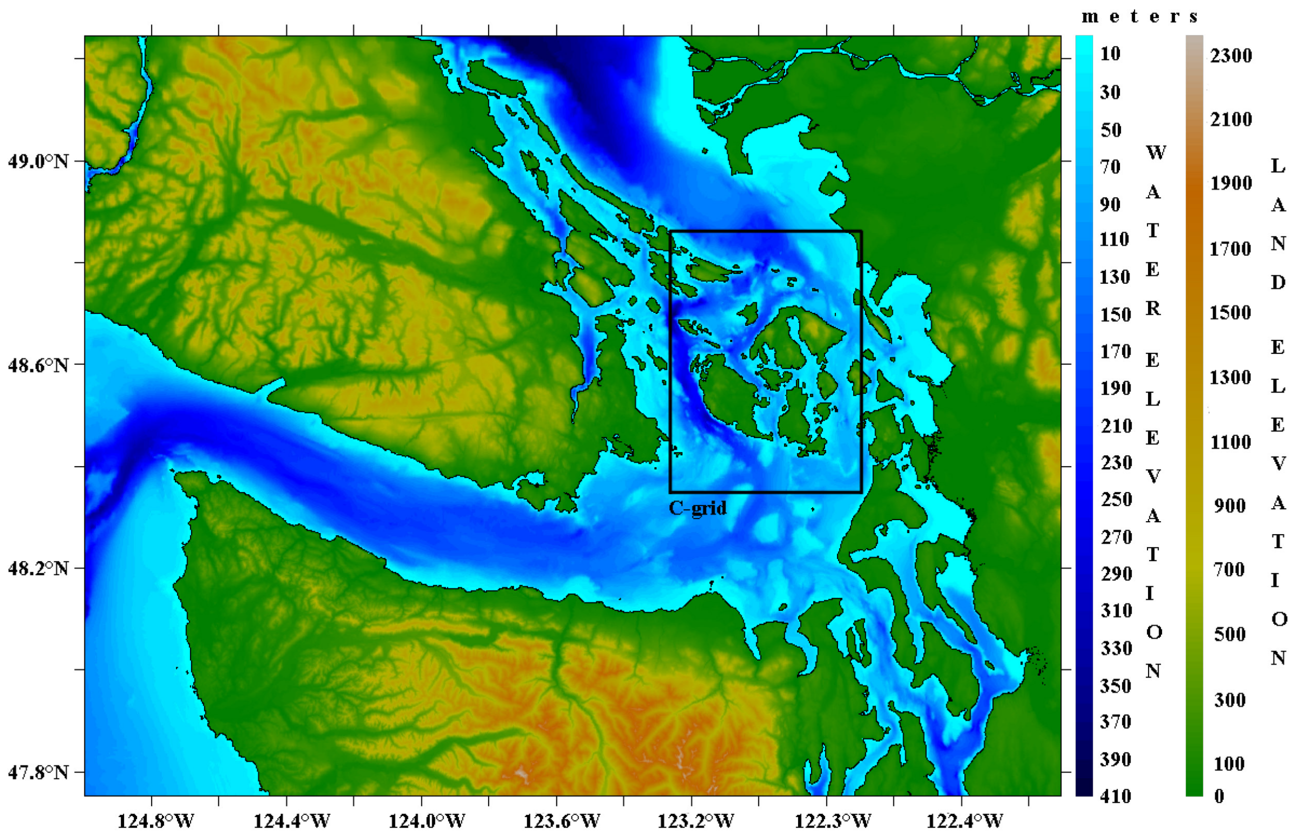

Figure 6. Extent of the B grid used for the San Juan Islands high-resolution inundation model. Black box indicates the extent of the C grid.

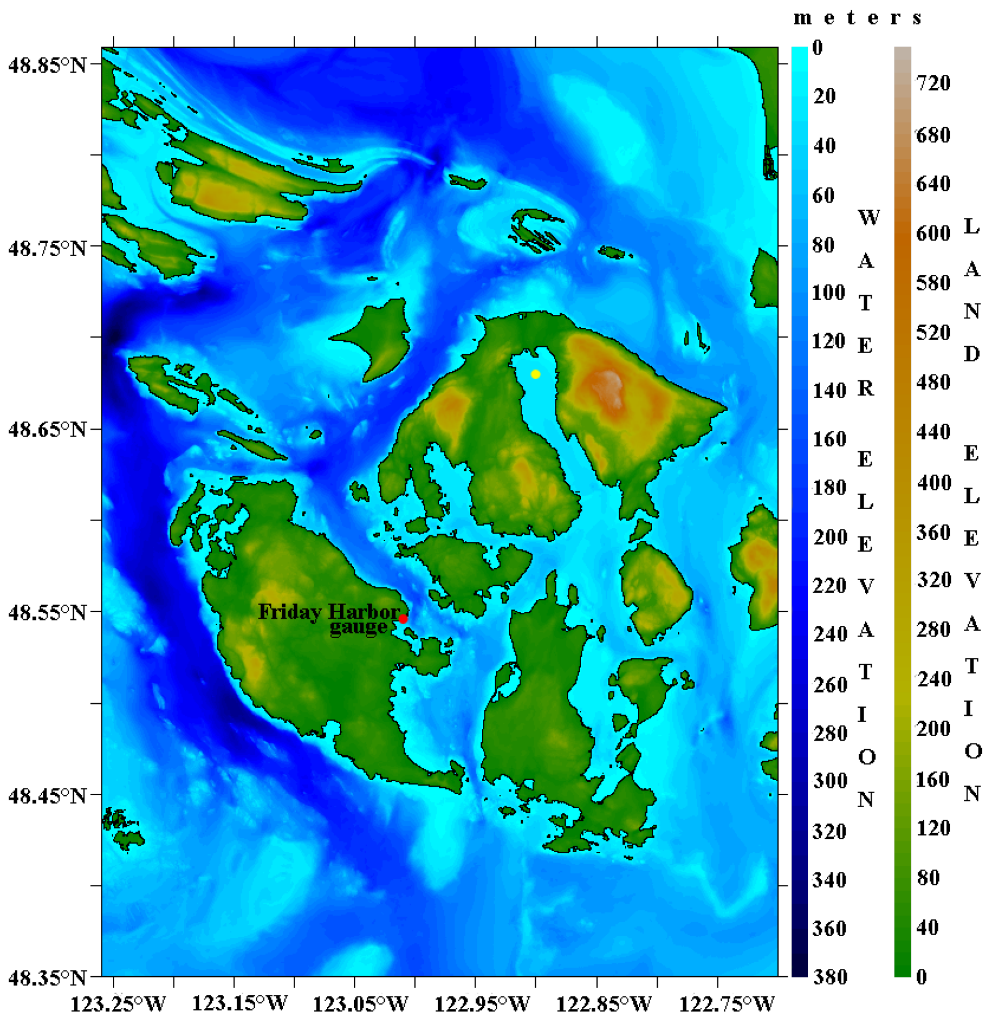

Figure 7. Extent of the C grid used for the San Juan Islands high-resolution inundation model. Red dot indicates the selected warning point at Friday Harbor (San Juan Island). The yellow dot indicates the selected point inside East Sound (offshore Orcas Island).

5. Model Results

This section discusses co-seismic deformation, and tsunami dynamics offshore and on the San Juan Islands' coasts based on simulated results from seismic source L1 (Witter et al., 2011).

5.1 Seismic deformation

Elevation of the bathymetry and topography is an important factor in conducting tsunami simulation; thus, if the seismic source is in the vicinity of the coastal area being studied, the seismic deformation should be taken into account. The MOST propagation code applies the deformation field of the earthquake onto the topographic and bathymetric grids before the tsunami is simulated.

The earthquake source Scenario L1 (Witter et al., 2011) causes uplift on the offshore region and subsidence along the coast of the Strait of Juan de Fuca (**Figure 3**). The extent of the co-seismic deformation due to Scenario L1 does not cover the San Juan Islands completely. The distribution of co-seismic deformation is plotted in **Figure 8**. The entire island of San Juan has a co-seismic subsidence of less than 15 cm while only portions of Orcas Island, Lopez Island, and Shaw Island have a co-seismic deformation of less than 10 cm; more than half of the C-grid is unaffected by co-seismic deformation. This is an important observation since ground subsidence due to co-seismic deformation will result in displacement of the coastline and permanent inundation of some areas. In this particular study, no major permanent inundation is expected in the San Juan Islands due to the small magnitude of co-seismic subsidence in the area.

5.2 Offshore dynamics

Due to the close proximity of the seismic source, the initial tsunami wave reaches the coast of Washington in less than 25 minutes. Complicated wave dynamics are generated after the initial tsunami wave hits the coast due to wave scattering and reflection, which can be clearly seen in **Figure 9** and in the A-grid animation (`SanJuanAgrid.mov`) provided in the **Supporting Information**. **Figure 9** plots the offshore wave dynamics at the A-grid level at 25 minute intervals. The wave front has reached most of the coastal areas of Washington and has entered the Strait of Juan de Fuca around 25 minutes after the earthquake (**Figure 9a**). At about 50 minutes, the tsunami wave front is inside the Strait of Juan de Fuca (**Figure 9b**). Due to the shallower water depths inside the Strait of Juan de Fuca, it takes longer than 1.25 hours before the initial wave front reaches the San Juan Islands (**Figure 9c**). The dynamics of the tsunami wave as it interacts with the San Juan archipelago is discussed in detail in section 5.3.

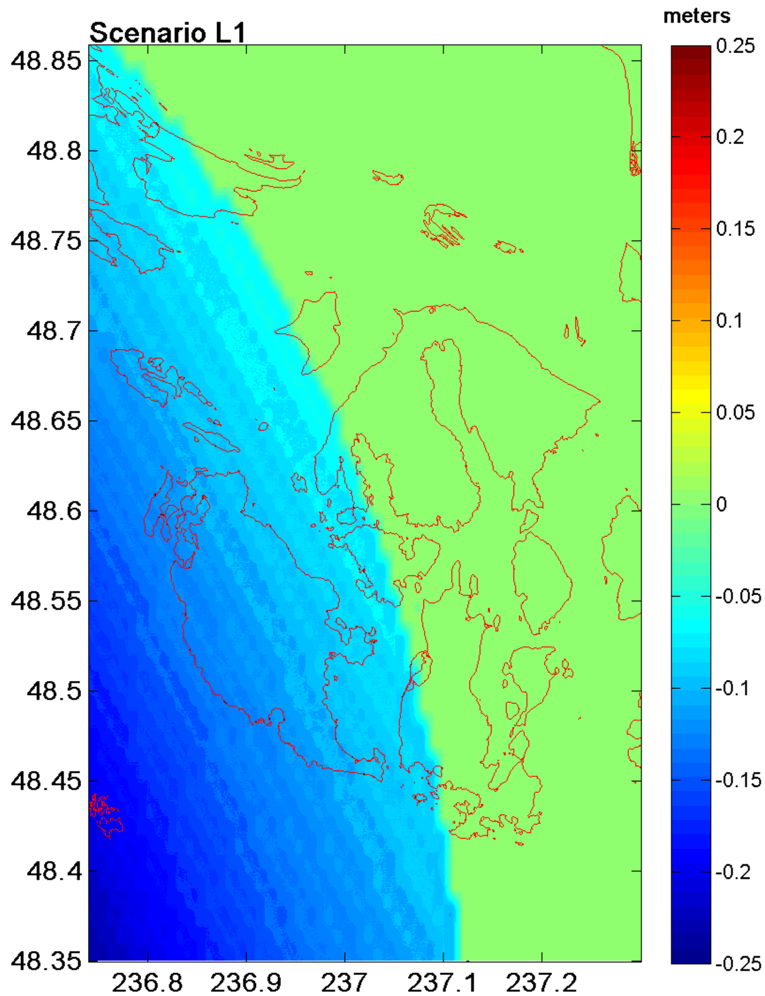

Figure 8. Co-seismic slip deformation at C-grid level for the San Juan Islands. A large portion of the C grid is not affected by the co-seismic deformation. Co-seismic changes to the shoreline are not noticeable at this scale.

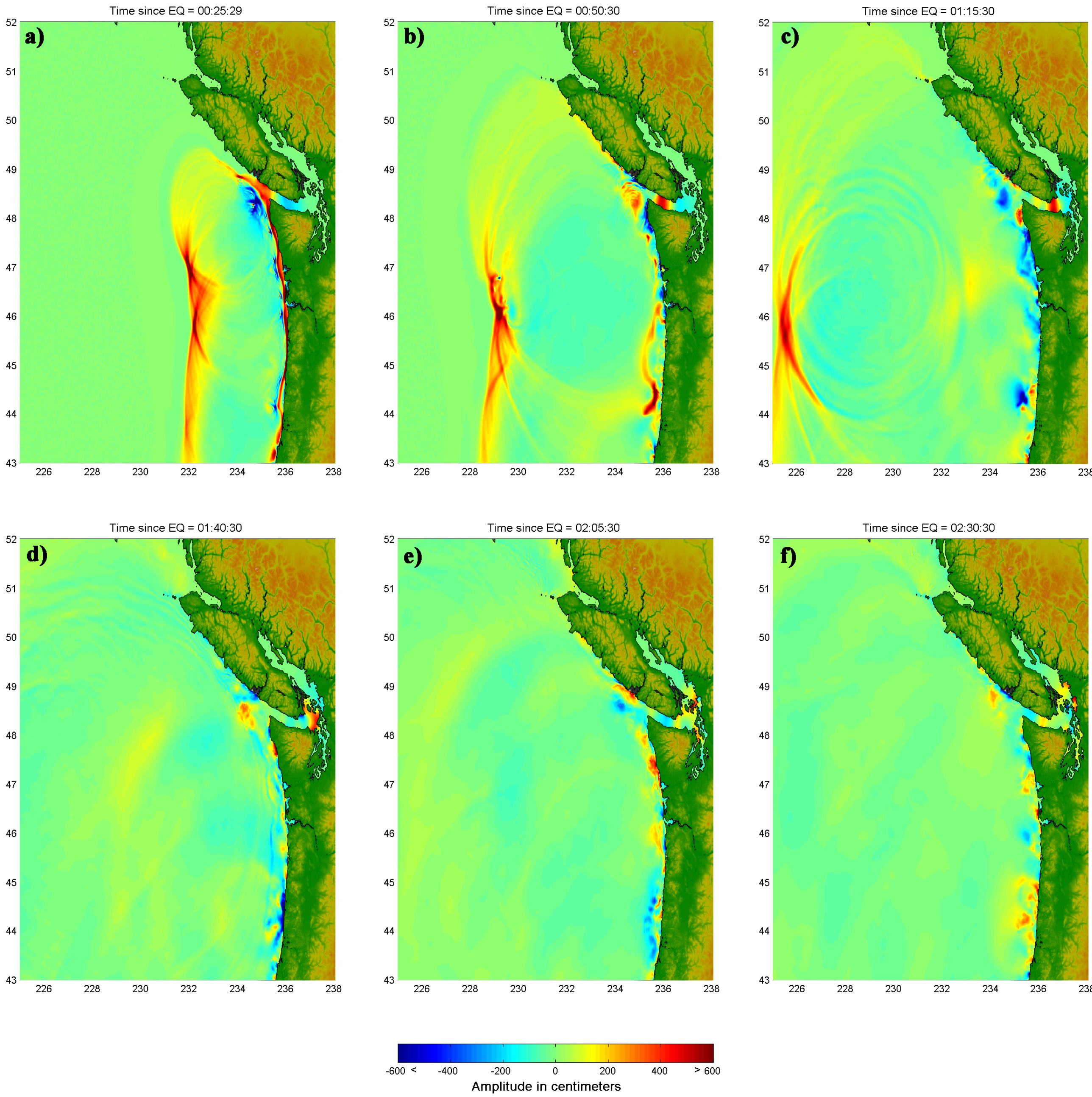

Figure 9. Modeled tsunami wave propagation on the offshore region of Washington for source L1. This is also the extent of the A grid. The frames are in approximately 25-minute intervals.

Wave trapping may occur along the continental shelf (Mofjeld et al., 2000); thus, the generated tsunami wave will continue for several hours, as illustrated in **Figure 9d–f**. This hazard assessment does not take into account the time at which this future event would occur with regard to low or high tide conditions. Thus, the study uses Mean High Water to simulate a scenario of maximum inundation along the coastline. The interpretation of simulated results should take into account that tidal effects and sea level rise are not included in the current study.

5.3 Tsunami dynamics and inundation

The incoming tsunami waves generated by source Scenario L1 hit the southern coast of San Juan Island first, then the southwest coast of Lopez Island. The waves continue to propagate along the eastern side of the San Juan Islands. Waves of lower amplitude propagate along the west coast of San Juan Island and Middle Channel entering into Griffin Bay and San Juan Channel. As the waves enter Upright Channel and West Sound (Orcas Island), the high waves that have propagated along the east side of the islands have spilled into the channels. These waves meet up and propagate further into the West Sound and East Sound of Orcas Island. Waves increase in amplitude as they get trapped on the southeast part of Lopez Island while the waves approaching East Sound (Orcas Island) build up. **Figure 10** plots the tsunami wave amplitude at different time steps as discussed. (An animation at the C-grid level, `SanJuanCgrid.mov`, is provided in the **Supporting Information**.) The selected time series point is close to the Friday Harbor tide gauge with coordinates of 236.99°E, 48.546°N and a depth of 2.08 m. The maximum tsunami amplitude at the Friday Harbor tide gauge is 2.49 m (**Figure 11**, top). A 10-hour simulation indicates that the tsunami wave height decreases after the arrival of the first maximum tsunami amplitude. The maximum current speed is about 30 cm/sec and does not coincide with the first maximum tsunami amplitude but occurs on the third wave (**Figure 11**, bottom). The largest computed wave elevation at the selected point (237.1°E, 48.68°N, depth of 26.1 m) in East Sound (Orcas Island) reaches 4.91 m with a maximum current speed of 40 cm/sec (**Figure 12**). Tsunami waves entering East Sound take several hours to settle, with later waves reaching smaller amplitudes around 1.5 m.

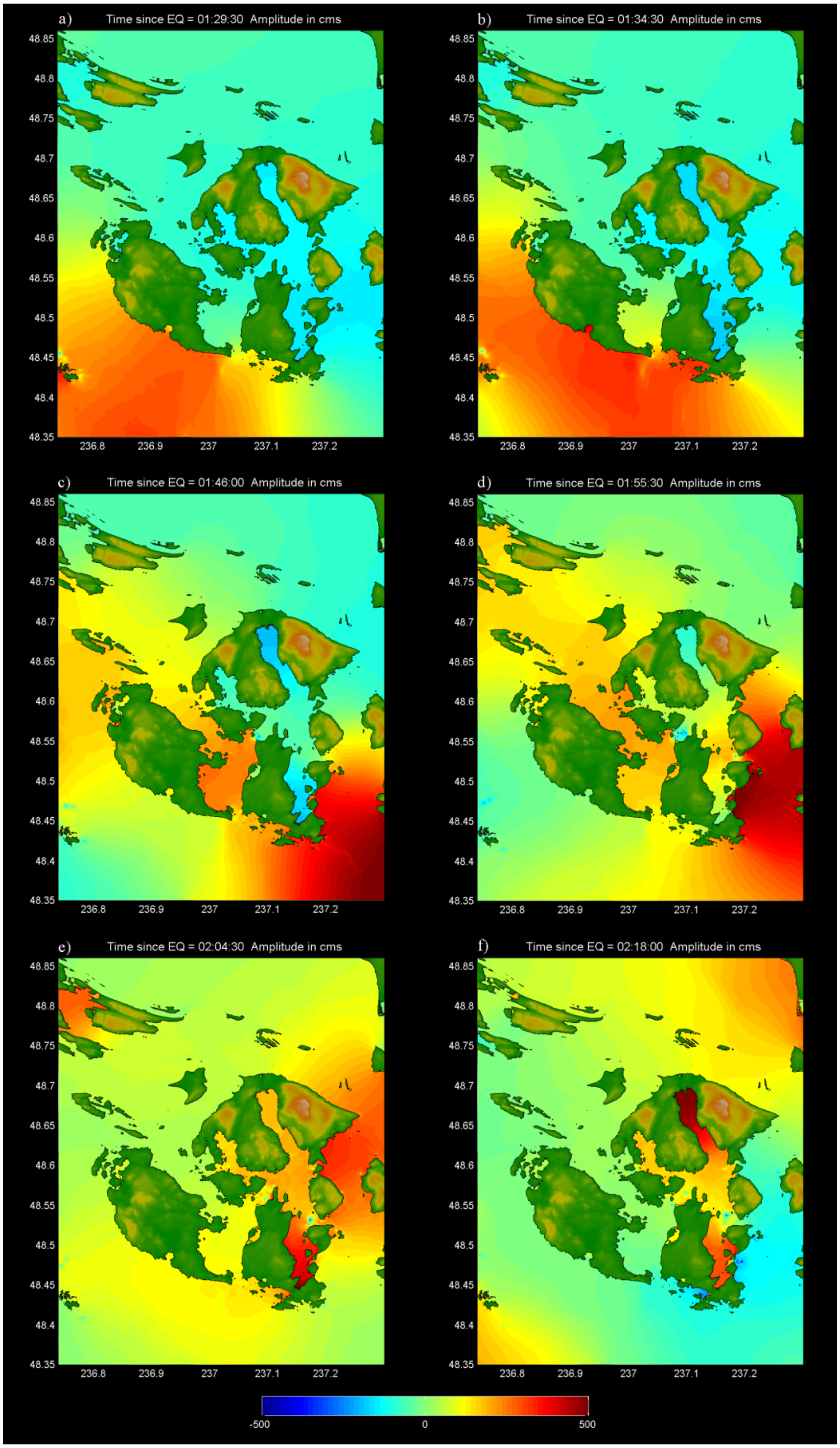

Figure 10. Propagating tsunami waves interacting with the San Juan Islands at the C-grid level.

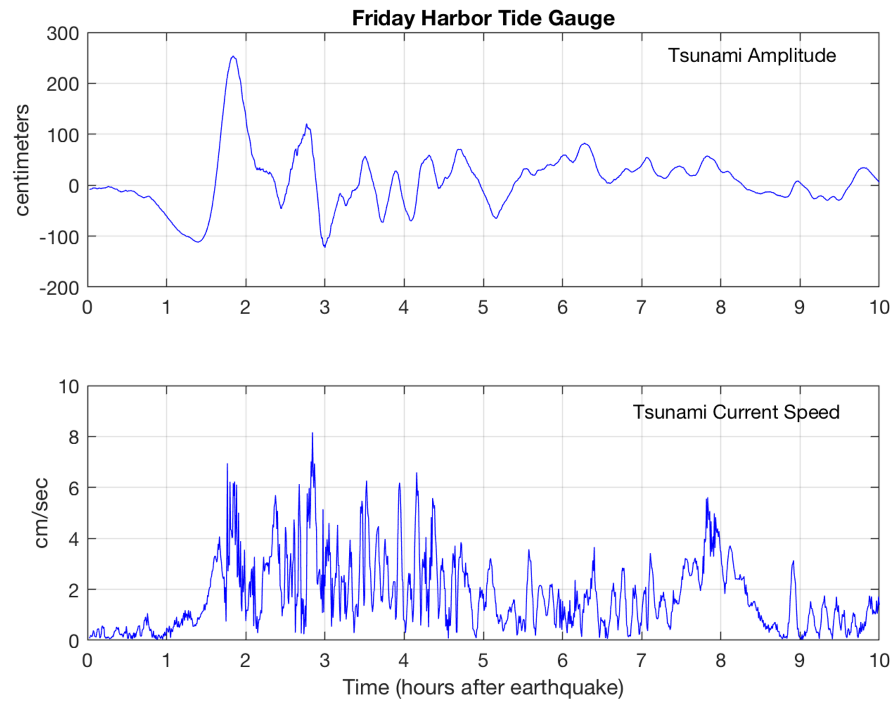

Figure 11. Simulated tsunami time series (upper panel) and current speed (lower panel) at the selected point (236.99°E, 48.546°N) for Friday Harbor (San Juan Island) based on source L1.

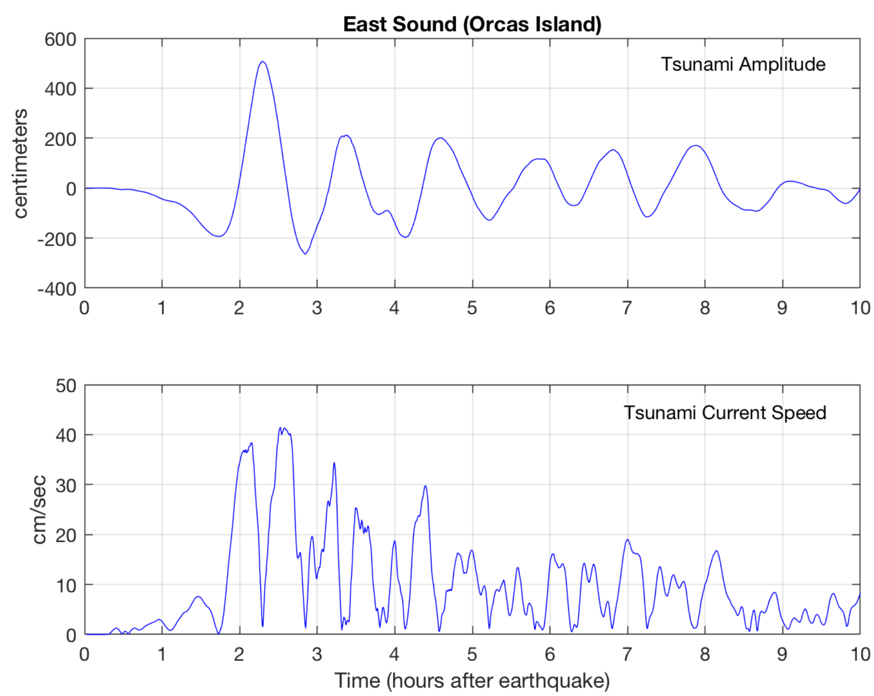

Figure 12. Simulated tsunami time series (upper panel) and current speed (lower panel) at the selected point (237.1°E, 48.68°N with 26.1 m depth) in East Sound (Orcas Island) based on source L1.

Figure 13, a plot of the maximum tsunami wave amplitude distribution, indicates that tsunami amplitude close to 5 m occurs in the East Sound area of Orcas Island. It also shows inundation occurring in some areas of Blakely Island, Decatur Island, San Juan Island, Lopez Island, Obstruction Island, Orcas Island, and Shaw Island. **Figures 14, 15,** and **16** illustrate flow depths for San Juan Island, Lopez

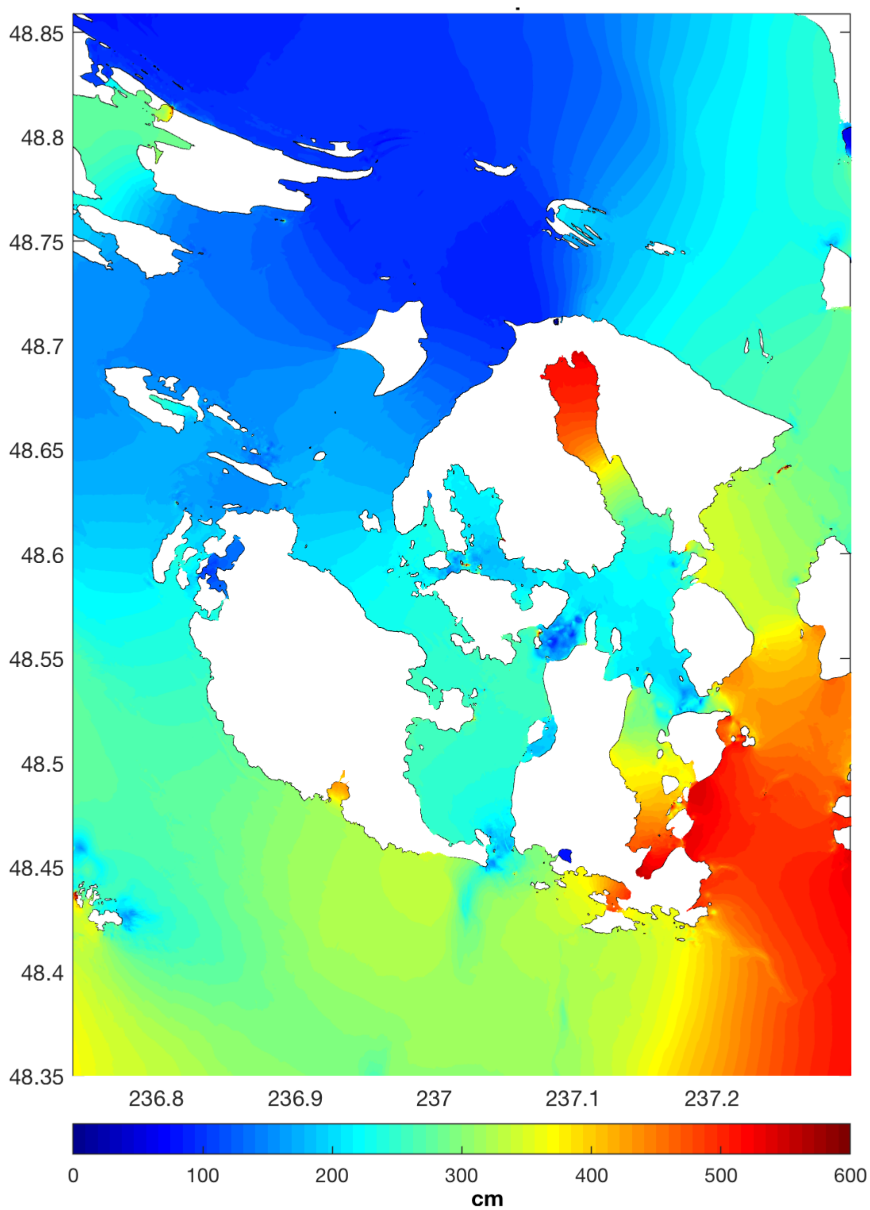

Figure 13. Maximum tsunami wave amplitude distribution for the San Juan Islands at the C-grid level based on source L1.

Island (including Decatur Island and Shaw Island), and Orcas Island (including Blakely Island and Obstruction Island), respectively. In terms of maximum tsunami current speed, most of the high current occurs along passages between the islands as shown in **Figure 17**. The velocity vectors are shown in **Figure 18**. Just before the tsunami wave front exits the Strait of Juan de Fuca and approaches the San Juan Islands, there is a drawdown as in the velocity vector field (**Figure 18a**, lower left corner) and the incoming tsunami wave front (**Figure 18b**, lower left corner). Strong velocities are seen occurring on the east side of San Juan Islands and in the channels between islands (**Figure 18c**); they continue to occur in the interior channels and passages (**Figure 18d–f**).

The formation of eddy structures is another important factor to consider, especially for navigation. (The formation of eddies in some channels can be seen in the **Supporting Information** C-grid animation SanJuanCgrid.mov.) Flow separation from geographical constrictions such as narrow passages will generate shear layers with large velocity gradients than can result in vortex shedding. The presence of these flow structures may pose a significant hazard to navigation through these narrow passages.

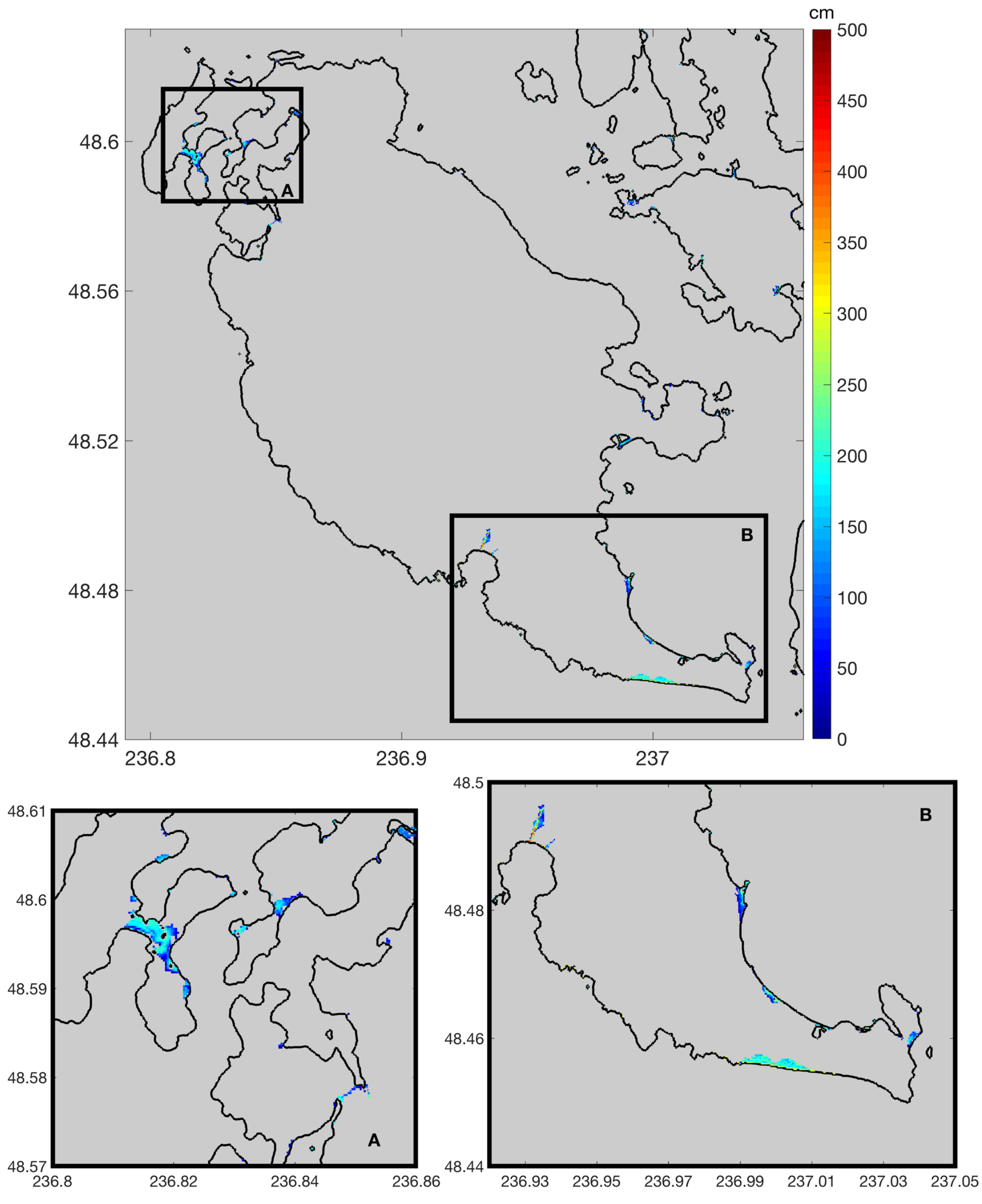

Figure 14. Extent of inundation and flow depth at San Juan Island. Given the large extension of the area covered in this study, the extent of inundated land appears to be relatively small at this scale. Panels A and B show more detail around the areas where the largest values of flow depth occur. Panel A shows inundated areas on Henry Island and Panel B those around South Beach. Inundated areas correlate well with low-lying topographic elevations impacted by a large tsunami wave.

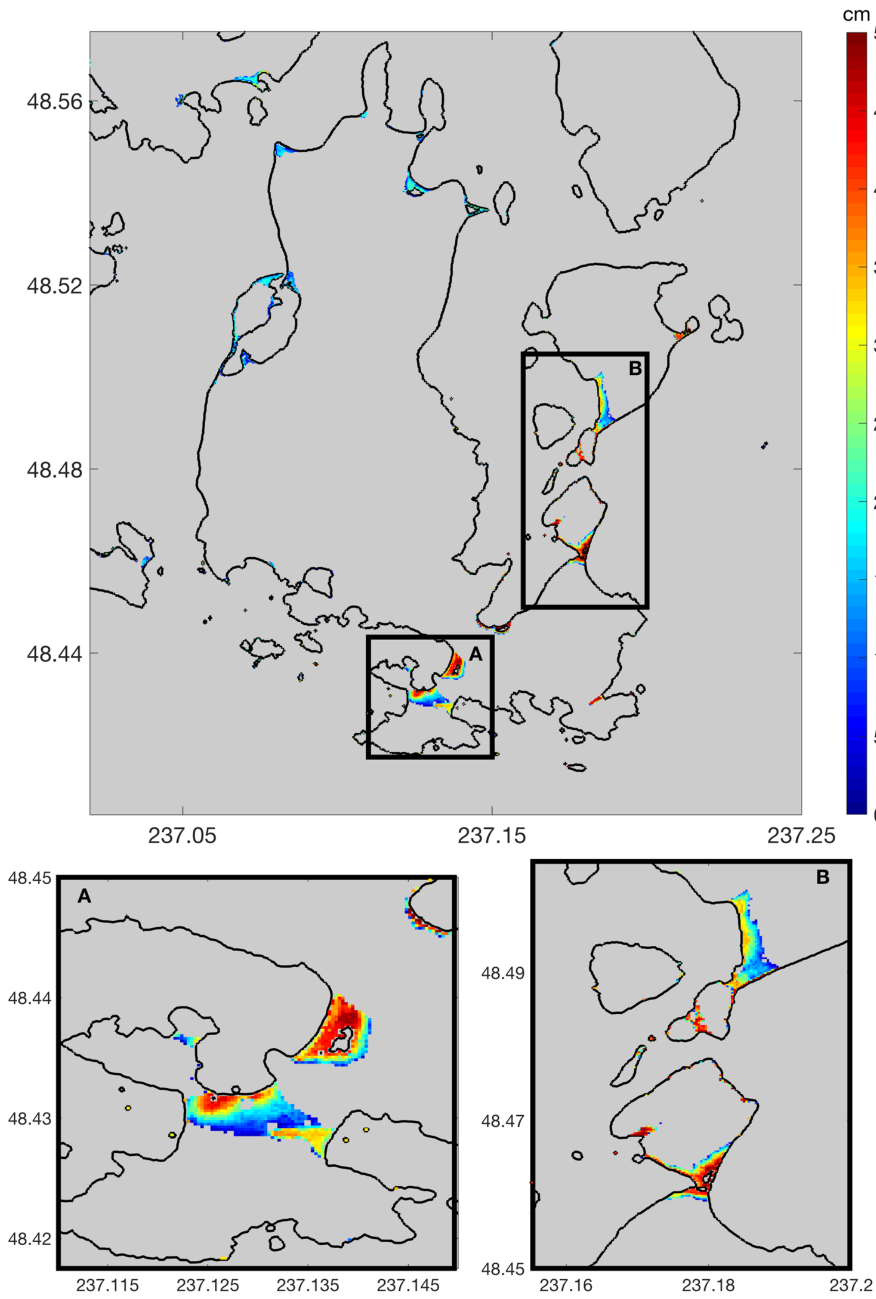

Figure 15. Extent of inundation and flow depth at Lopez, Decatur, and Shaw Islands. Given the large extension of the area covered in this study, the extent of inundated land appears to be relatively small at this scale, Panels A and B show more detail around the areas where the largest values of flow depth occur. Panel A shows flow depth in Mackaye Harbor and Barlow Bay, and Panel B in the Gerring Beach area in the southern tip of Decatur Island and in the isthmus between Shoal and Mud Bay. Inundated areas correlate well with low-lying topographic elevations impacted by a large tsunami wave.

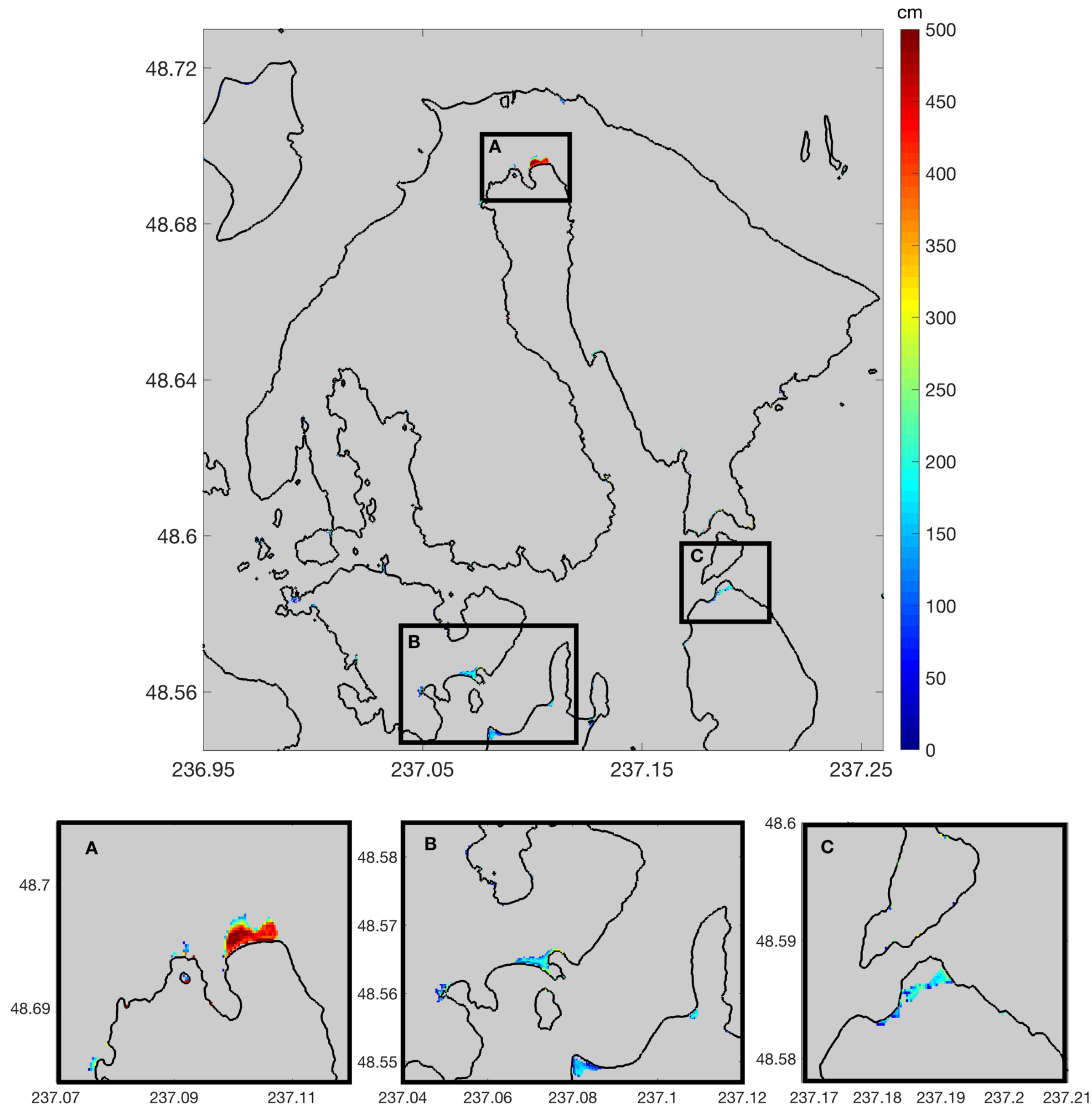

Figure 16. Extent of inundation and flow depth at Orcas Island. Given the large extension of the area covered in this study, the extent of inundated land appears to be relatively small at this scale. Panels A, B, and C show more detail around the areas where the largest values of flow depth occur, namely Eastsound (Panel A), some inundated areas along the southern coast of Shaw Island and the northern coast of Lopez Island (Panel B), and along the northern tip of Blakely Island. Inundated areas correlate well with low-lying topographic elevations impacted by a large tsunami wave.

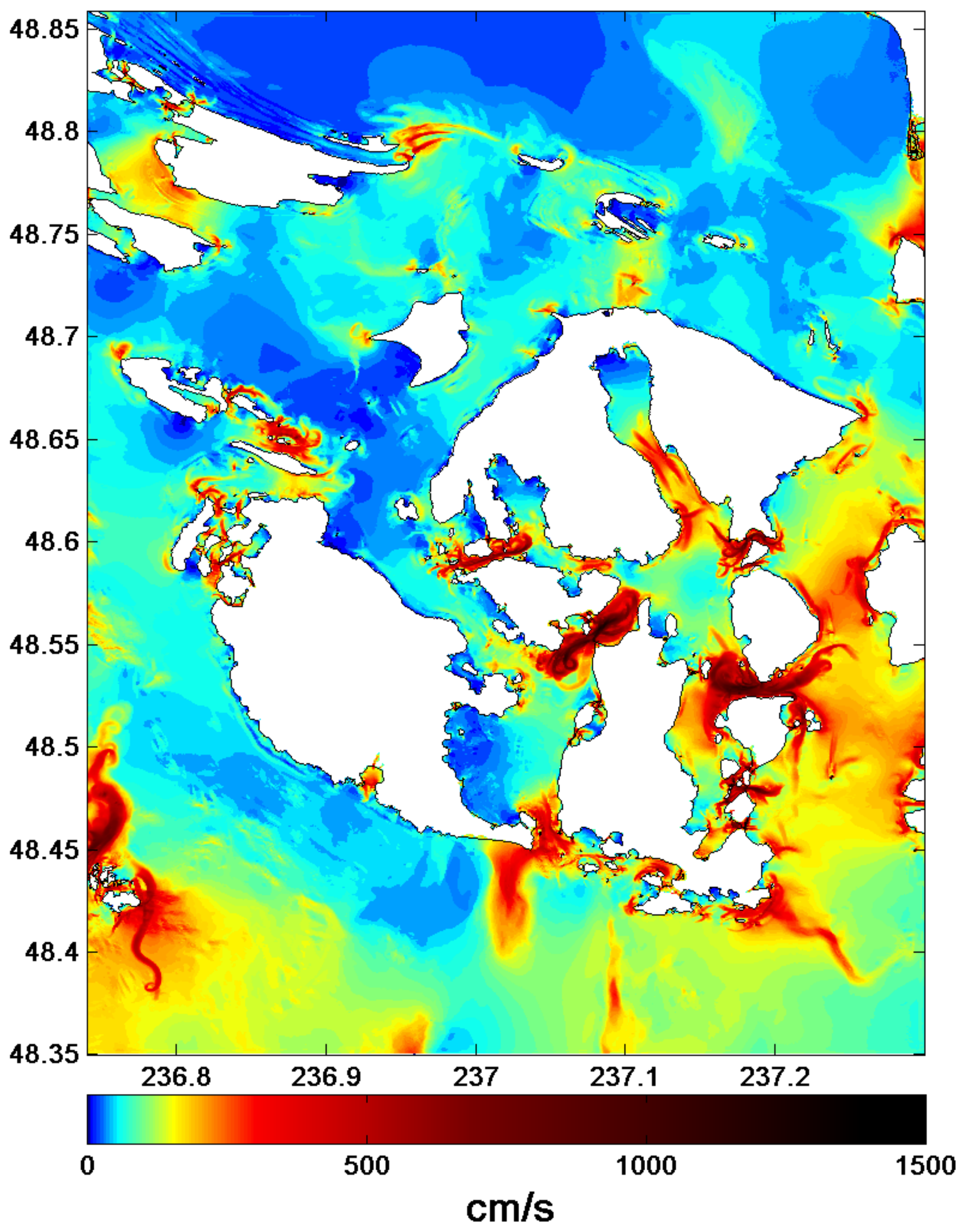

Figure 17. Maximum tsunami wave current distribution for the San Juan Islands at the C-grid level based on source L1 with higher current distribution, especially in the channels.

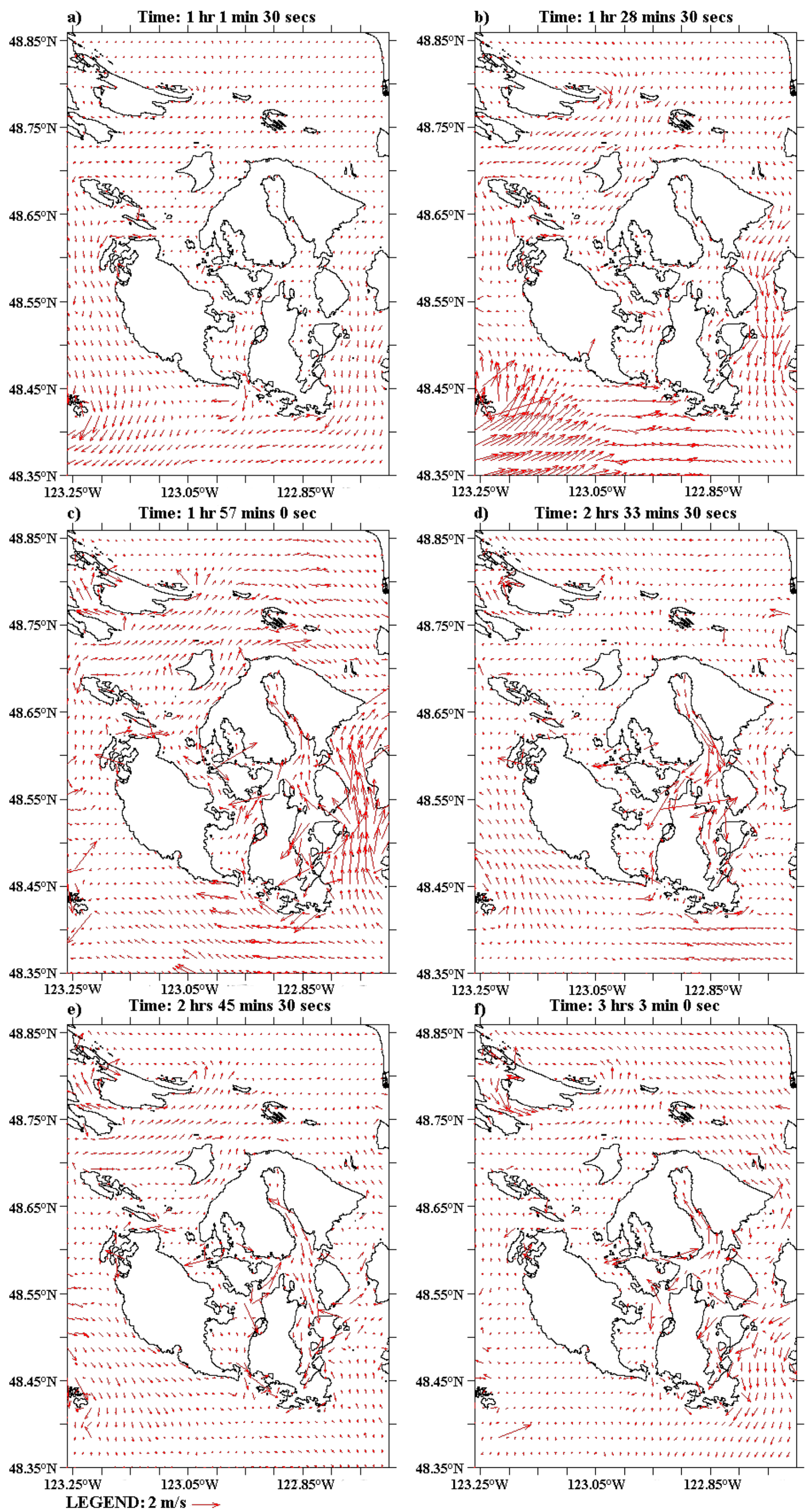

Figure 18. Velocity vectors at different time frames after the earthquake.

6. Summary

An earthquake source, scenario L1, developed by Witter et al. (2011) was used to model a Cascadia subduction zone source tsunami for the San Juan Islands, Washington. A high-resolution inundation model with three nested grids was developed, based on a 0.4 arc-second DEM developed by NGDC (Lim et al., 2011). The simulated results show that it takes more than 1.25 hours before the tsunami wave front hits the southern parts of the San Juan Islands. The wave front then proceeds to travel around the islands, in both directions, and at the same time enters the passages between the islands, spilling into the bays and sounds inside the archipelago.

Due to the location of the San Juan Islands and the size of earthquake source scenario L1 (Witter et al., 2011), the co-seismic deformation is minimal and does not affect the entire San Juan Islands area. The largest co-seismic deformation for San Juan Island is only 15 cm and less than 10 cm on portions of Orcas Island, Lopez Island, and Shaw Island. Overall, the shoreline change is negligible or nonexistent. Based on this simulated scenario, the inundation will only be temporary, caused by run-up and withdrawal processes associated with the tsunami waves and not by seismic subsidence of the terrain.

The maximum tsunami wave amplitude at the Friday Harbor (San Juan Island) sample point is 2.49 m with a maximum current speed of 30 cm/sec. The highest simulated tsunami wave amplitude occurs at the north end of East Sound (Orcas Island) measuring 4.91 m with a current speed of 40 cm/sec. The later waves of the tsunami die out quickly at Friday Harbor while they take several hours in East Sound, as illustrated in the simulated tsunami series plotted in **Figures 11** and **12**, respectively. Inundation occurs at some areas on Blakely Island, Decatur Island, San Juan Island, Lopez Island, Obstruction Island, Orcas Island, and Shaw Island. The simulated flow depth can be as high as 3 m or more at certain locations of Decatur Island, Lopez Island (**Figure 15**), and Orcas Island (**Figure 16**). High currents occur in passages between islands, as plotted in **Figure 17** and as shown in the velocity vector plots in **Figure 18**. One important item to note, especially for navigation, is the formation of eddies in some of the channels.

Interpretation of the simulated results for San Juan Islands should consider that the modeling approach implemented in the study does not include the effects of tides. This study does not take into account the particular state of the tide at the time of tsunami arrival. In order to obtain a conservative estimate of inundation and run-up, the simulated results presented here are based on Mean High Water for maximum tsunami impact. The Mean High Water used in the current study is 4.27 feet above Mean Sea Level (Tides and Currents, 2013). Sea level rise is another factor not considered in this study. The predicted scenario along the coast of Washington yields a sea level rise of 0 to 1 ft per century (Climate Program Office, 2012).

Acknowledgments

This publication is contribution 4069 from NOAA/Pacific Marine Environmental Laboratory and is [partially] funded by the Joint Institute for the Study of the Atmosphere and Ocean (JISAO) under NOAA Cooperative Agreement No. NA10OAR4320148, Contribution No. 2172. Special thanks to Marie Eblé for her assistance in updating online references.

References

Arcas, D., E. Gica, and V.V. Titov. Tsunami inundation modeling of Long Beach and Ocean Shores, Washington, due to a Cascadia Subduction Zone Earthquake. [Unpublished study]

Atwater, B.F., and E. Hemphill-Haley (1997). Recurrence intervals for great earthquakes of the past 3,500 years at northeastern Willapa Bay, Washington. U.S. Geological Survey Professional Paper 1576. Prepared in cooperation with the Nuclear Regulatory Commission. U.S. Government Printing Office, Washington, D.C.

Atwater, B.F., et al. (1995). Summary of coastal geologic evidence for past great earthquakes at the Cascadia Subduction Zone. *Earthq. Spectra, 11*(1), 1–18.

Atwater, B.F., S. Musumi-Rokkaku, K. Satake, Y. Tsuji, K. Ueda, and D.K. Yamaguchi (2005). The orphan tsunami of 1700—Japanese clues to a parent earthquake in North America. U.S. Geological Survey Professional Paper 1707. University of Washington Press, Seattle, WA.

Bureau of Land Management (Accessed June 2019). San Juan Island National Monument. https://www.blm.gov/programs/national-conservation-lands/national-monuments/oregon-washington/san-juan-islands

Climate Program Office (2012). Global sea level rise scenarios for the United States National Climate Assessment. Climate Program Office, NOAA Technical Report OAR CPO-1.

Dengler, L., et al. (2011). Learning from Earthquakes: The Japan Tohoku Tsunami of March 11, 2011. EERI Special Earthquake Report—November 2011. Earthquake Engineering Research Institute, Oakland, CA.

Goldfinger, C., et al. (2012). Turbidite event history—Methods and implications for Holocene paleoseismicity of the Cascadia subduction zone. U.S. Geological Survey Professional Paper 1661-F. https://doi.org/10.3133/pp1661F

Graehl, N., H.M. Kelsey, R.C. Witter, E. Hemphill-Haley, and S.E. Engelhart (2015). Stratigraphic and microfossil evidence for a 4500-year history of Cascadia subduction zone earthquakes and tsunamis at Yaquina River estuary, Oregon, USA. *Geol. Soc. Amer. Bull., 127*(1-2), 211–226. https://doi.org/10.1130/B31074.1

Kelsey, H.M., A.R. Nelson, E. Hemphill-Haley, and R.C. Witter (2005). Tsunami history of an Oregon coastal lake reveals a 4600 yr record of great earthquakes on the Cascadia subduction zone. *Geol. Soc. Amer. Bull., 117*(7-8), 1009–1032. https://doi.org/10.1130/B25452.1

Lim, E., L.A. Taylor, B.W. Eakins, K.S. Carignan, M.R. Love, P.R. Grothe, and D.Z. Friday (2011). Digital elevation models of San Juan Islands, Washington: Procedures, data sources and analysis. NOAA National Geophysical Data Center Report, 37 pp.

McLellan, R.D. (1927). *The Geology of the San Juan Islands.* University of Washington Publications in Geology. University of Washington Press, Seattle, WA. Available at https://www.nps.gov/parkhistory/online_books/geology/publications/state/wa/uw-1927-2/contents.htm

Mofjeld, H.O., V.V. Titov, F.I. González, and J.C. Newman (2000). Analytic theory of tsunami wave scattering in the open ocean with application of the North Pacific Ocean, NOAA Technical Memorandum, OAR PMEL-116, NTIS: PB2002-101562, 38 pp.

National Park Service. (Accessed June 2019). San Juan Island National Historical Park, Washington. https://www.nps.gov/sajh/learn/index.htm

Nelson, A.R., H.M. Kelsey, and R.C. Witter (2006). Great earthquakes of variable magnitude at the Cascadia subduction zone. *Quaternary Res., 65*(3), 354–365. https://doi.org/10.1016/j.yqres.2006.02.009

Orcas Island Chamber of Commerce (Accessed 2019). https://orcasislandchamber.com/orcas-island

Petersen, M.D., C.H. Cramer, and A.D. Frankel (2002). Simulations of seismic hazard for the Pacific Northwest of the United States from earthquakes associated with the Cascadia Subduction Zone. *Pure Appl. Geophys., 159*(9), 2147–2168.

Puget Sound Partnership (Accessed 2019). Shared strategy for Puget Sound: Watershed profile. https://www.psp.wa.gov/shared-salmon-strategy/watersheds/watershed-sanjuan.htm#Stats

San Juan Islands Visitors Bureau (Accessed June 2019). https://www.visitsanjuans.com/

Satake, K., K. Shimazaki, Y. Tsuji, and K. Ueda (1996). Time and size of a giant earthquake in Cascadia inferred from Japanese tsunami records of January 1700. *Nature, 379*(6562), 246–249. https://doi.org/10.1038/379246a0

Satake, K., K. Wang, and B.F. Atwater (2003). Fault slip and seismic moment of the 1700 Cascadia earthquake inferred from Japanese tsunami descriptions. *J. Geophys. Res., 108*(B11), 2535. https://doi.org/10.1029/2003JB002521

Synolakis, C.E., E.N. Bernard, V.V. Titov, U. Kânoğlu, and F.I. González (2007). Standards, criteria, and procedures for NOAA evaluation of tsunami numerical models. NOAA Technical Memorandum, OAR PMEL-135, NOAA/Pacific Marine Environmental Laboratory, Seattle, WA, 55 pp.

Tides and Currents (Accessed October 25, 2013). https://tidesandcurrents.noaa.gov/datums.html?id=9441102

Titov, V.V., and F.I. González (1997). Implementation and testing of the Method of Splitting Tsunami (MOST) model. NOAA Technical Memorandum ERL PMEL-112, NTIS: PB98-122773, NOAA/Pacific Marine Environmental Laboratory, Seattle, WA, 11 pp.

Titov, V.V., and C.E. Synolakis (1998). Numerical modeling of tidal wave runup. *J. Waterw. Port Coast. Ocean Eng., 124*(4), 157–171.

Tolkova, E. Method Of Splitting Tsunamis (MOST) model, version 4. [Unpublished study]

Tucker, B., and T. King (2012). San Juan County, Washington, Community Wildfire Protection Plan. Report for San Juan County and the Bureau of Land Management, Northwest Management, Inc., Moscow, ID. 105 pp.

U.S. Census Bureau (Accessed 2019). Quick Facts, San Juan County. https://www.census.gov/quickfacts/sanjuancountywashington

U.S. Congress (2011). *Congressional Record–Senate: Proceedings and Debates of the 112th Congress, First Session, Vol. 157 Part 10, September 14, 2011*. US Government Printing Office, Washington, D.C., p. 13,582.

Vance-Sherman, A. (Accessed 2020). San Juan County profile. Employment Security Department, State of Washington. https://esd.wa.gov/labormarketinfo/county-profiles/san-juan

Venturato, A.J., V.V. Titov, H.O. Mofjeld, and F.I. González (2004). NOAA TIME eastern Strait of Juan de Fuca, Washington mapping project: Procedures, data sources, and products. NOAA Technical Memorandum OAR PMEL-127, NTIS: PB2005-101207, Seattle, Washington, 22 pp.

Witter, R.C., H.M. Kelsey, and E. Hemphill-Haley (2003). Great Cascadia earthquakes and tsunamis of the past 6700 years, Coquille River estuary, southern coastal Oregon. *Geol. Soc. Amer. Bull., 115*(10), 1289–1306.

Witter, R.C., Y. Zhang, K. Wang, G.R. Priest, C. Goldfinger, L.L. Stimely, J.T. English, and P.A. Ferro (2011). Simulating tsunami inundation at Bandon, Coos County, Oregon, using hypothetical Cascadia and Alaska earthquake scenarios, Special Paper 43. Oregon Department of Geology and Mineral Industries, 63 pp.

Witter, R.C., Y.J. Zhang, K. Wang, C. Goldfinger, and G.R. Priest (2012). Coseismic slip on the southern Cascadia megathrust implied by tsunami deposits in an Oregon lake and earthquake-triggered marine turbidites: *J. Geophys. Res., 117,* B10303. https://doi.org/10.1029/2012JB009404

Witter, R.C., J.J. Yinglong, Y.J. Zhang, K.R. Wang, G.T. Priest, L.A. Stimely, J. English, P.A. Ferro, and C. Goldfinger (2013). Simulated tsunami inundation for a range of Cascadia megathrust earthquake scenarios at Bandon, Oregon, USA. *Geosphere, 9*(6), 1783–1803.

Yamaguchi, D.K., B.F. Atwater, D.E. Bunker, B.E. Benson, and M.S. Reid (1997). Tree-ring dating in the 1700 Cascadia Earthquake. *Nature, 389*(6654), 922–924.

Supporting Information

D. Arcas[1], E. Gica[2], and V. V. Titov[1]

Animations (SanJuanAgrid.mov, SanJuanBgrid.mov, SanJuanCgrid.mov, and SanJuanIslandsCgridSpeed.mov) showing the impact on the San Juan Islands, Washington, of a tsunami generated by a hypothetical Mw 9.0 subduction zone event along the Cascadia margin for grids A, B, and C have been posted at https://nctr.pmel.noaa.gov/animate.html and published on the NOAAPMEL YouTube channel playlist, *Hypothetical Cascadia tsunami: San Juan Islands, WA* (https://www.youtube.com/playlist?list=PLRA00iWmFaKa1dfDQ-XSvss56h9jr4KOo).

Table S1: List of products provided.

Product Name	Description
Animation	Tsunami wave evolution and amplitude of source scenario L1 at A-, B-, and C-grid levels for the San Juan Islands. Tsunami speed at C-grid level.
Documentation	Modeling product report.
ASCII MOST	ASCIIs MOST format of DEM (un-deformed and deformed) used in the simulation, maximum tsunami wave amplitude, and current distributions and flow depth at C-grid level.
GIS	Geospatial representation of model results in ESRI ArcGIS and ASCII raster format for maximum tsunami wave amplitude and current distributions and flow depth for C grid.
Images	Images of DEM, model results, and time series.
KMZ	Zipped KML files of maximum tsunami wave amplitude and current distributions and flow depth.
Time series	Text file of model time series at Friday Harbor and East Sound.

1 NOAA Center for Tsunami Research, Pacific Marine Environmental Laboratory (PMEL), NOAA, Seattle, WA

2 Formerly at University of Washington, Joint Institute for the Study of the Atmosphere and Ocean, Seattle, WA